

# ACTUAL RADIAL WIDTH OF CUT AND CUTTING MODE IN 2<sup>1/2</sup>-D SPIRAL-OUT POCKETING

Y. S. Ma<sup>1</sup>, S. Hinduja<sup>2</sup> and G. Barrow<sup>3</sup>

## ABSTRACT

This paper describes a method to calculate the variation in the radial width of cut which occurs when the cutter travels a spiral-out toolpath in pocketing. This variation is approximated by a stepped curve, thus enabling each segment of the toolpath to be divided into several subsections, the radial width remaining constant over each subsection. The method also enables the cutting mode to be determined. By using this method, it is possible to optimize pocketing operations more precisely and to achieve near optimal cutting conditions. An example is included where the actual radial width of cut are calculated.

## INTRODUCTION

The goal of CAM systems is to achieve minimum machining cost or production rate by fully utilising the potential capacity of cutting tools and the machine. Technological constraints, such as maximum cutting force, chip capacity, chattering and surface finish, must be taken into consideration. For a CAM system, such as TECHMILL (Lau 1987), tool selection and the optimization of cutting conditions are inter-linked in order to minimize the machining cost or time (see Fig.1). In order to optimize the cutting conditions, it is necessary to know the exact cutting geometry. For example, in milling, radial width and axial depth of cut are basic geometrical parameters to choose appropriate cutting velocity and feed rates.

In 2<sup>1/2</sup>-D pocketing, the depth of cut is a constant, the actual radial width of cut is then the major parameter required to predict the cutting force. When using spiral-out tool paths, the distance between two neighbouring cutting passes is a constant. It can be appreciated that the actual radial width of cut still changes considerably from place to place. For example, it has been reported (Kline 1982) that the cutting force can increase by more than a factor of ten when cutting corners. Such critical regions may cause chatter or tool breakage. Wang (Wang 1988) suggested that the feed rate should be changed according to the "in-process part geometry" so that the cutting force is under control.

Since different cutting modes, such as up milling,

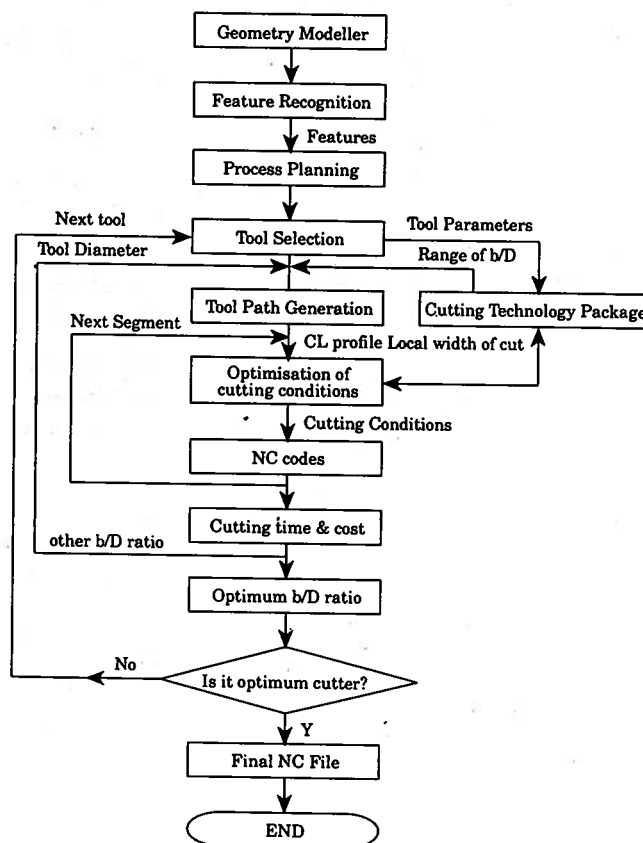


Fig 1 Overview of the TECHMILL System.

down milling, slotting and symmetrical milling, affect tool life considerably (Lau 1987), the cutting mode should also be considered in the optimization of cutting conditions. 3-D simulation systems for NC milling have been available (Hook 1986 and Wang 1986). However, most of them are used for graphical collision check, actual cutting geometries are not calculated. A few systems (Wang 1988, Wang 1987, Takata 1989, and Bouzakis 1992) can simulate cutting geometries for each cutter motion, the computing time is too long to be used in optimization procedures.

In this work, a simple method has been developed to calculate the actual radial width of cut and determine the cutting mode in 2<sup>1/2</sup>-D pocketing. A procedure catering for spiral-out tool paths has been implemented.

<sup>1</sup> Lecturer, Department of Mechanical Engineering, Ngee Ann Polytechnic, 535 Clementi Road, Singapore 2159.

<sup>2</sup> Senior Lecturer, Manufacturing Division, Department of Mechanical Engineering, UMIST, P.O. Box 88, Manchester, M60 1QD, UK.

<sup>3</sup> Senior Lecturer, Manufacturing Division, Department of Mechanical Engineering, UMIST, P.O. Box 88, Manchester, M60 1QD, UK.

## CUTTER SWEEPED AREA

Suppose the tool path consists of straight lines and circular arcs. The cutter swept area of a given segment is the area enclosed by the envelope curve which is generated when the cutter travels from the start point to the end point of the segment.

The swept area of the cutter travelling along a straight line segment is shown in Fig. 2. If the cutter moves from  $P_1$  to  $P_2$ , then  $\overline{P_{o1}P_{o2}}$ ,  $\overline{P_{o2}P_{m2}P_{i2}}$ ,  $\overline{P_{i2}P_{i1}}$  and  $\overline{P_{i1}P_{m1}P_{o1}}$  compose the boundary of the swept area. Suppose the cutter's moving vector is  $\vec{E}$ , the pocket boundary normal vector is  $\vec{S}$ , then the Outer Bound (OB) is the offset of the given CL segment on the side represented by the vector  $\vec{C}_2$  ( $\vec{C}_2 = -\vec{S} \times \vec{E}$ ). Whereas the Inner Bound (IB) is the offset of the given CL segment on the side represented by the vector  $\vec{C}_1$  ( $\vec{C}_1 = \vec{S} \times \vec{E}$ ). In Fig. 2,  $\overline{P_{o1}P_{o2}}$  is the OB of the swept area,  $\overline{P_{i2}P_{i1}}$  the IB.  $\overline{P_{o2}P_{m2}P_{i2}}$  and  $\overline{P_{i1}P_{m1}P_{o1}}$  are referred to as the Penetration Arc (PA) and the Touching Arc (TA) of the swept area respectively. Point  $P_{o1}$ ,  $P_{i1}$  are referred to as the initial and the end points of the swept area respectively because the OB starts from  $P_{o1}$  and the IB ends at  $P_{i1}$ .

It should be noted that for the first tool path segment, the start point of the segment is the start point of the pocket machining, therefore, the area enclosed by the cutter circle at the start point is part of the swept area as well, i.e. the swept area is  $P_{i1}P_{m11}P_{o1}P_{o2}P_{m2}P_{i2}P_{i1}$  (see Fig. 2). Similarly, the cutter swept area travelling along a circular arc segment can be constructed.

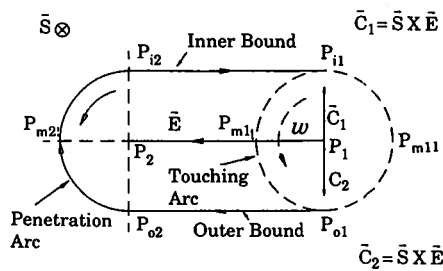


Fig 2 Cutter swept area.

## CURRENT SWEEPED AREA AND DERIVATION OF MACHINED AREA

When the cutter travels along the tool path, i.e. the cutter Centre Location (CL) profile, the work material enclosed in the cutter swept area is removed segment by segment. The area that has already been machined is referred to as the machined area. It is the envelope of all the swept areas which have been generated by the cutter. The boundary of the machined area is represented as a graph in the solid modeller, hence it is referred to as machined graph. The machined graph develops as the cutter traverses each CL segment. The relative position between the machined graph and the current swept area determines the cutting geometry, i.e. the cutting mode and the actual width of cut. Diagrams showing both the machined graph and the current swept area are referred to as the

Cutting Geometry Diagrams (CGD). Obviously, as the cutting process continues, the CGD for each instant changes continuously.

A simple example is given in Fig. 3. The pocket boundary is ABCDEFGH, the tool path is shown in Fig. 3(a), the start point is  $P_1$ . The swept area, after the cutter traverses the first CL segment on the tool path  $P_1P_2$ , is shown in Fig. 3(b) (i.e.  $A_1B_1C_1D_1E_1F_1A_1$ ). It is also the machined area for the next CL segment. Obviously, the cutting mode for the first CL segment is slotting. When the cutter moves from  $P_2$  to  $P_3$ , the material enclosed by the new swept area ( $P_{o2}P_{o3}P_{m3}P_{i3}P_{i2}$ ) is removed. Along this CL segment, the cutter moves from the inner layer cutting pass to the next outer layer cutting pass. Fig. 3(b) shows the CGD when the cutter traversing CL segment  $P_2$  to  $P_3$ . The cutting mode for this segment is a combination of down milling and slotting. The current swept area intersects with the machined graph at points  $G_1$  and  $F_1$ . The cutting starts with the down milling mode, then the radial width of cut increases gradually, until it changes to slotting when the cutter touches  $G_1$ .

After traversing CL segment  $P_2P_3$ , the machined graph is updated to  $H_1I_1G_1B_1C_1D_1E_1F_1H_1$ , which

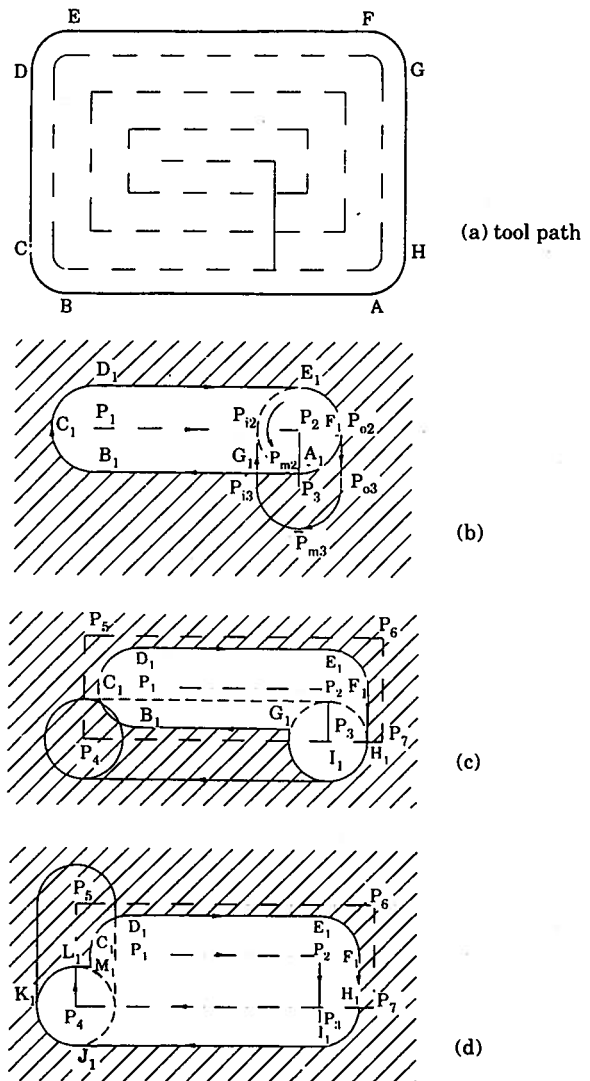


Fig 3 Derivation of the machined graph.

is shown in Fig. 3(c). Fig. 3(c) is the CGD of the next CL segment  $P_3 P_4$ . By traversing  $P_3 P_4$ , the new machined graph is derived as  $J_1 K_1 L_1 M_1 C_1 D_1 E_1 F_1 H_1 I_1 J_1$  shown in Fig. 3(d). By traversing the tool path segment by segment, the machined graph is derived step by step, hence the CGD corresponding to the new CL segment can be obtained.

To calculate the real width of cut and to analyze the cutting mode, the Cutting Geometry Diagrams (CGDs) need to be studied. It is first necessary to classify these CGDs so that the underlying characteristics of CGDs may be investigated.

### CLASSIFICATION OF CGDS

It is the authors' observation that when the cutter is effectively removing work material, then the boundary of the swept area must intersect with the machined graph. In this work, the classification of CGDs is based on the patterns of these intersection points along the boundary of the cutter swept area.

It can be appreciated that the Touching Arc has no intersection point with the machined graph. It is either partially coincident with a segment of the machined graph or enclosed completely by the machined graph. So the Touching Arc is not considered when considering intersection between the boundary of the current swept area and the machined graph. The intersection points must be distributed along the OB, PA and IB. Where they lie reflects the cutting geometry. Sometimes, more than one intersection point lies on one segment of the swept envelope (Fig. 4), while sometimes different intersection points are on different segments (Fig. 5). It is assumed that at most there are two intersection points on a single swept area curve, and at most there are two separated areas to be machined within a swept area (Fig. 4). It appears that such an assumption is too rigid to deal with practical pocket machining, but according to the simulation tests performed, it is good enough for spiral-out pocketing.

Several critical logical variables are used to represent the pattern of the cutting geometry.

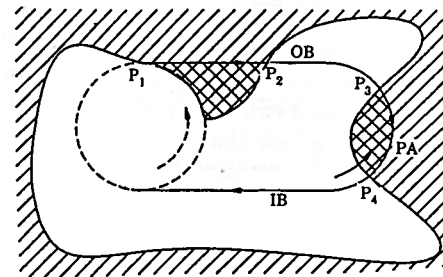
**TINSIDE** : True, when the cutter is completely in the machined graph at the start point of the current CL segment and it is not touching the machined graph. False, otherwise.

**TINSID1** : True, when the cutter is completely in the machined graph at the end point of the current CL segment. False, otherwise.

**OBINTER** : True, when there is any intersection point on the OB of the current swept area. False, otherwise.

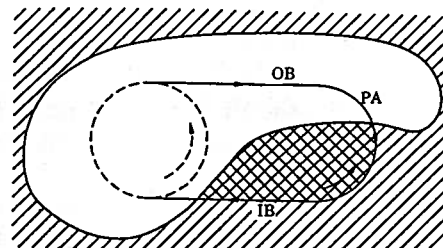
**OBINTE1** : True, when there are two intersection points on the OB of the current swept area. False, otherwise.

**IBINTER** : True, when there is any intersection point on the IB of the current swept area. False, otherwise.



TINSIDE=F      TINSID1=F      OBINTER=T      OBINTE1=F  
 IBINTER=F      IBINTE1=F      PAINTER=T      PAINTE1=T  
 CUTTING MODES: 3+4+5 (DOWN MILLING + CUTTING AIR + SYMMETRICAL MILLING)

Fig 4 An example of cutting geometry diagram (CGD).



TINSIDE=T      TINSID1=F      OBINTER=F      OBINTE1=F  
 IBINTER=T      IBINTE1=F      PAINTER=T      PAINTE1=F  
 CUTTING MODES: 4+2 (CUTTING AIR + UP MILLING)

Fig 5 An example of cutting geometry diagram (CGD).

**IBINTE1** : True, when there are two intersection points on the IB of the current swept area. False, otherwise.

**PAINTER** : True, when there is any intersection point on the PA of the current swept area. False, otherwise.

**PAINTE1** : True, when there are two intersection points on the PA of the current swept area. False, otherwise.

Obviously, different combinations of these logical variables may occur, but under the assumptions discussed above, the number of possible CGDs is quite limited. Therefore it is possible to implement a procedure to analyze these limited number of CGDs. For example, in Fig.4, the CGD is represented by "OBINTER=T PAINTER=T PAINTE1=T others=F", in Fig. 5, the CGD is represented by "TINSIDE=T IBINTER=T PAINTER=T others=F". In the following table, some common cases represented by different value combinations of the logical variables are given. (Table 1).

### UPDATING OF THE MACHINED GRAPH

In order to obtain correct CGDs, when simulating the cutter's traversing along the CL profile, segment by segment, the machined graph has to be updated continuously. Basically, two procedures are needed, i.e. creating the newly generated segments on the machined graph and the removing invalid old segments.

Table 1

CASE	TINSIDE	TINSID1	OBINTER	OBINTE1	IBINTER	IBINTE1	PAINTER	PAINTE1
1	T	F	F	F	F	F	F	F
2	F	F	F	F	F	F	F	F
3	F	F	F	F	F	F	T	F
4	T	F	F	F	F	F	T	T
5	F	T	T	F	F	F	F	F
6	T	T	T	T	F	F	F	F
7	T	F	T	F	F	F	T	F
8	F	F	T	F	F	F	T	T
9	F	F	T	T	F	F	T	F
10	F	F	F	F	T	F	F	F
11	T	T	F	F	T	T	F	F
12	F	F	F	F	T	F	T	T
13	F	F	F	F	T	T	T	F
14	T	F	F	F	T	F	T	F
15	F	F	T	T	T	F	F	F
16	F	T	T	F	T	T	F	F
17	T	F	T	F	T	F	F	F
18	F	F	T	F	T	F	T	F
19	T	F	T	T	T	F	T	F
20	T	F	T	F	T	F	T	T
21	T	F	T	F	T	T	T	F

### (a) Removal of Unwanted Segments

Those segments of the old machined graph, enclosed in the current swept area, are unwanted, and to be removed. After obtaining the intersection points between the current swept area and the old machined graph, all the intersection points are queued according to their distances from the initial point along the swept area boundary. Then starting with the first intersection point, the old machined graph is traversed in the direction of entering the current swept area, until next intersection point is encountered, then the segments traversed are detected as unwanted segments and removed.

Within the swept area, there could be two chains of segments belonging to the old machined graph, hence such a removal procedure may be executed twice if there are four intersection points in the queue.

For example, in Fig. 4,  $P_1, P_2, P_3, P_4$  are four intersection points, the first chain of unwanted segments is the one starting from  $P_1$ , and ending at  $P_2$  in the swept area. The second chain is the one from  $P_3$  to  $P_4$  in the swept area.

### (b) Creation of the Newly Generated Segments

The newly generated segments of the machined graph are those along the boundary of the swept area and not enclosed by the old machine graph. They are chained from one intersection point to another intersection point so that the machined graph profile is closed up. For example, in Fig. 4,  $P_1 P_2$  (part of OB) and  $P_3 P_4$  (part of PA) are two newly generated segments on the machined graph.

The new segments on the machined graph is constructed by traversing the swept area boundary

and copying those segments which satisfy the above condition, to the machined graph. The traversing and the copying process starts from the intersection point nearest to the initial point along the swept area boundary, then the process goes on until the next intersection point is encountered. If there are another two intersection points, the same procedure is then executed again. In Fig. 4,  $P_1, P_2$  are linked with the straight line in the machined graph, while  $P_3, P_4$  are linked with an arc.

### CUTTING MODES

Traditionally, cutting modes in milling include: slotting, down-milling, up-milling etc. These concepts originated from manual milling practice. However, more cutting modes may be encountered, and Lau (Lau 1987) has analyzed them in some detail. In this work, cutting geometries are classified into seven cutting modes (Fig. 6): (a) down milling, (b) up-milling, (c) slotting, (d) symmetrical milling, (e) pro-down milling, (f) pro-up-milling and (g) both sides cutting – combination of up-milling and down-milling modes.

Actually, this classification is based on the understanding of the cutter tooth sweeping process with the consideration of cutting force direction, entry and exit angles, and effective chip thickness. Obviously, where the cutter tooth enters the work material (cutter entry point) and where it leaves the work material (cutter exit point) determine the above parameters.

In this work, the cutting modes are defined according to the position of the cutter entry point and the cutter exit point. The cutter tooth swept semi-circle is partitioned into four zones (Fig. 7), i.e. zone 1, zone 2, zone 3 and zone 4.

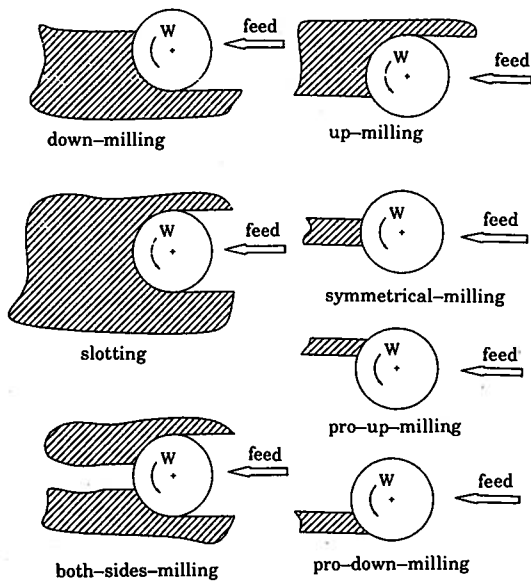


Fig 6 Different cutting modes.

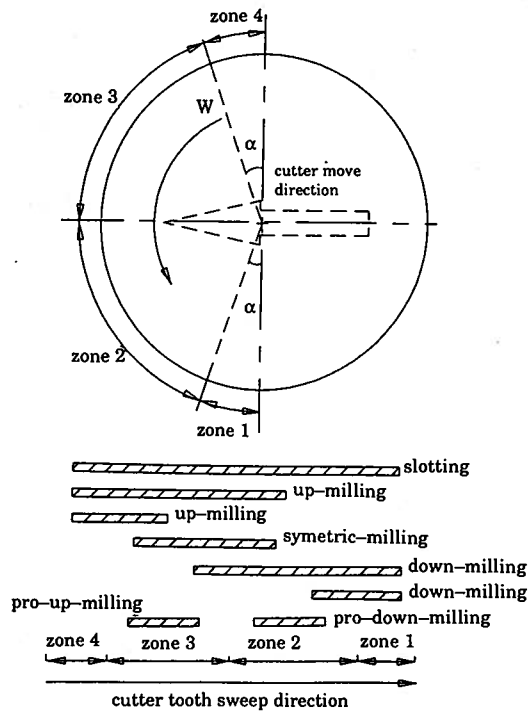


Fig 7 Classification of cutting modes.

Some typical examples of different cutting modes are illustrated in Fig. 7 with different horizontal bars representing the cutter tooth swept ranges. It should be noted that the traditional definitions of cutting modes are quite rigid, e.g. in slotting, both the cutter tooth entry and exit angles must be  $0^\circ$ . However, in order to cover more varieties of cutting modes encountered in milling with the applications of CAD/CAM systems, a more flexible definition is needed.

- if the entry point falls in zone 4, and the exit point falls in zone 1, then the cutting modes is defined as slotting.
- if the entry point falls in zone 4, and the exit point falls in either zone 4, zone 3, or zone 2, then the cutting mode is defined as up-milling.

- if the exit point falls in zone 1, and the entry point falls in either zone 3, zone 2, or zone 1, then the cutting mode is defined as down-milling.
- if the entry point falls in zone 3, and the exit point falls in zone 2, then the cutting mode is defined as symmetrical-milling.
- if both the entry point and the exit point fall in zone 3, then the cutting mode is defined as pro-up-milling.
- if both the entry point and the exit point fall in zone 2, then the cutting mode is defined as pro-down-milling.
- The cutting mode in which up-milling and down-milling modes are combined, is then defined as both-sides-milling.

The most suitable value for  $\alpha$  is a matter for discussing. Currently, it is set to  $30^\circ$ .

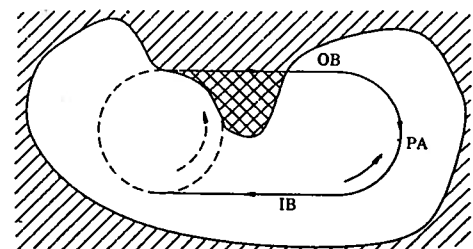
### DETERMINATION OF THE CUTTING MODE BY ANALYSING CGDS

Assuming that there is only one stock area enclosed in the cutter swept area. As mentioned previously, the positions of the entry point and the exit point of the stock profile, (i.e. where the stock profile enters and exits the cutter swept area) determine the cutting mode to machine the stock area. The relationship can be described in the following table: (Table 2).

Sometimes, more than one stock area is enclosed in the cutter swept area, then the combined cutting mode may occur. In this work, the stock areas are analyzed individually. After calculating the real width of cut

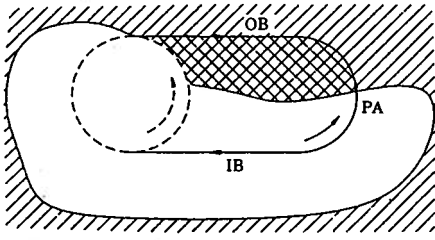
Table 2

If the entry points is on	If the exit point is on	Cutting mode	Example figure
OB	OB	down-milling	Fig. 8
OB	PA	down-milling	Fig. 9
OB	IB	down/up milling+ slotting	Fig. 10
PA	PA	pro-down/up or sym. milling	Fig. 11
PA	IB	up-milling	Fig. 5
IB	IB	up-milling	Fig. 12



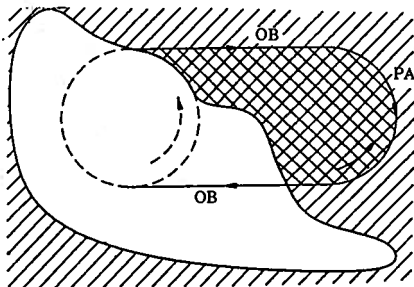
TINSIDE=F TINSID1=F OBINTER=T OBINTE1=F  
 IBINTER=F IBINTE1=F PAINTER=F PAINTE1=F  
 CUTTING MODES: 3+4 (DOWN MILLING + CUTTING AIR)

Fig 8 An example of cutting geometry diagrams.



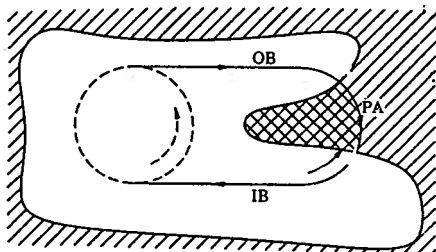
TINSIDE=F    TINSID1=F    OBINTER=F    OBINTE1=F  
 IBINTER=F    IBINTE1=F    PAINTER=T    -PAINTE1=F  
 CUTTING MODES: 3

Fig 9 An example of cutting geometry diagrams.



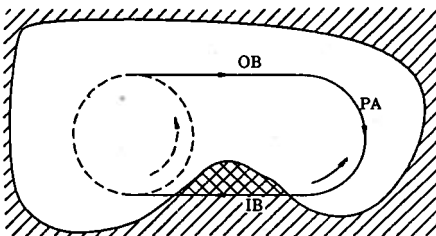
TINSIDE=F    TINSID1=F    OBINTER=F    OBINTE1=F  
 IBINTER=T    IBINTE1=F    PAINTER=F    PAINTE1=F  
 CUTTING MODES: 3+1 (DOWN MILLING + SLOTTING)

Fig 10 An example of cutting geometry diagrams.



TINSIDE=T    TINSID1=F    OBINTER=F    OBINTE1=F  
 IBINTER=F    IBINTE1=F    PAINTER=T    PAINTE1=T  
 CUTTING MODES: 4+5 (CUTTING AIR + SYMMETRICAL MILLING)

Fig 11 An example of cutting geometry diagrams.



TINSIDE=T    TINSID1=T    OBINTER=F    OBINTE1=F  
 IBINTER=T    IBINTE1=T    PAINTER=F    PAINTE1=F  
 CUTTING MODES: 4+2+4 (CUTTING AIR + UP MILLING + CUTTING AIR)

Fig 12 An example of cutting geometry diagrams.

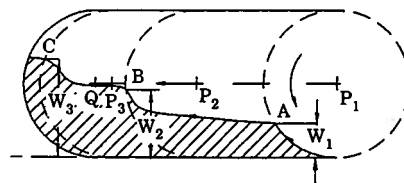
### CALCULATION OF THE REAL WIDTH OF CUT

Although the concept of width of cut is commonly used in practice, but it has no strict definition for different cutting modes. A general description can be that:

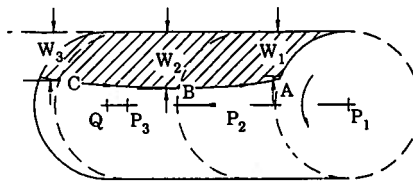
For a given cutting position, there could be several pairs of entry and exit points along the cutter's circumference at which the cutter cuts into and leaves the work material. For each pair, calculate the distance between the entry and exit points in the direction perpendicular to the feed vector. Then the width of cut at this cutting position is the sum of all these distances.

For the cases where there are more than one pair of entry/exit points present at a position, the width of cut is calculated pair by pair. Hence, the following discussion is limited to the cases with only one pair of entry/exit points.

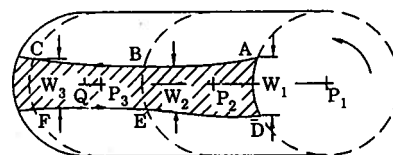
In Fig. 13, three cutting modes are shown when the cutter traversing a straight line CL segment from  $P_1$  to  $Q$ . In Fig. 13(a), the cutting mode is down-milling. The hatched area is the material to be removed. A, B, C are three points on the machined graph and are enclosed in the current swept area. The cutter reaches A, B and C when its centre is at  $P_1$ ,  $P_2$  and  $P_3$  respectively. The width of cut changes continuously as the cutter moves along the CL segment. The width of cut in the down-milling mode is the distance from the entry point to the outer bound of the current swept area or its extension. In Fig. 13(a), when the cutter reaches position  $P_1$ , the entry point is A, the distance from A to the outer bound is  $w_1$ , so  $w_1$  is the width of cut. Similarly,  $w_2$  and  $w_3$  are the widths of cut when the cutter is at positions  $P_2$  and  $P_3$  respectively.



(a) down milling



(b) up-milling



(c) symmetrical milling

Fig 13 Actual radial widths at different positions (Straight line segments).

for each stock area, the effective width of cut and cutting mode are then determined by merging different stock areas' widths of cut and cutting modes. The detailed merging method is presented in the next section.

In Fig. 13(b), the cutting mode is up-milling. The width of cut in this cutting mode is the distance from the exit point to the inner bound of the current swept area or its extension. For example, A is the exit point when the cutter is at position  $P_1$ , the distance from point A to the inner bound, i.e.  $w_1$  is the width of cut at that cutting position. When the cutter centre reaches point  $P_2$  and  $P_3$ , the widths of cut are  $w_2$  and  $w_3$  respectively.

In Fig. 13(c), the cutting mode is symmetrical milling. For a given cutter position, draw parallel lines of the cutter CL segment from the entry and exit point respectively, then the width of cut is the distance between these two parallel lines.  $w_1$ ,  $w_2$  and  $w_3$  represent the widths of cut when the cutter is at position  $P_1$ ,  $P_2$ , and  $P_3$  respectively. Similarly, this definition of the width of cut is also applicable for a circular CL segment.

**(a) Approximation of Stock Profile by using Step-Wise Stock Profile**

It should be noted that the actual width of cut may change for every cutter motion, if it is calculated for every motion, the computational time will be extensive. Due to this reason, in this work, the width of cut is determined in steps. Cutting conditions can also be calculated step-wise.

In order to do so, stock profiles enclosed in the current swept area are simplified into step-wise profiles, i.e. for each small segment on the stock profile, the maximum width of cut is used as the constant width of cut for the corresponding CL segment. For example, in Fig. 14(a), an original stock profile is shown. It is simplified as the step-wise profile shown in Fig. 14(b) in which the stock widths at each step are indicated. Then the question is how to convert the stock widths to the widths of cut between different cutting positions?

Although the stock profile has been simplified as a step-wise profile, there are still some transient periods

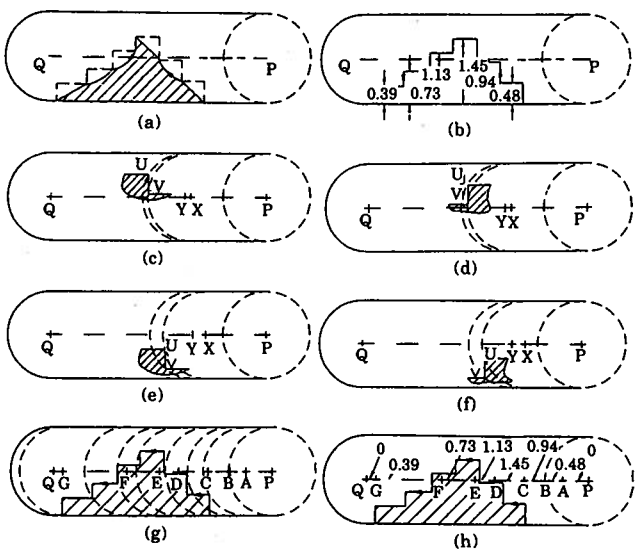


Fig 14 The calculation of the actual radial width of cut.

need to be treated specially. Such transient periods correspond to the vertical segments on the step-wise profile. Again, in this work the width of cut during such transient periods is assumed to be constant, the maximum value is used. For example, in Fig. 14(c), the cutter reaches point V first when the cutter centre is at position X, then the width of cut increases gradually. When the cutter reaches point U, i.e. the cutter centre is at position Y, and the width of cut becomes the maximum in this transient period. Then, this maximum width of cut is used as the constant width of cut for this transient period from X to Y. In Fig. 14(d), when the cutter moves from position X to Y, it reaches V first again, but the actual width of cut decreases gradually until the cutter reaches U. In this case the width of cut when the cutter is centred at position X, is used for the cutting period from X to Y. Similarly, for the cutting period from X to Y in Fig.14(e), the instant width of cut at position Y is used as the constant width of cut, while in Fig. 14(f), the instant width at position X is used.

Next, the original CL segment is split at the corresponding cutter centre positions for different steps, every newly generated CL segment is related to a step, i.e. it has a constant width of cut. In Fig. 14(g), small CL segments and their corresponding cutter swept arcs are shown. Fig.14(h) shows the corresponding widths of cut.

In the above example, the cutting mode is down milling, it is straight forward to apply a similar technique to deal with up-milling. For symmetrical milling, more attention is needed (Fig. 15). Since in symmetrical milling, neither the entry point nor the exit point of the cutter is on the boundary of the swept area. The stock profile within the current swept area changes its direction, i.e. it has a U turn. For a given cutting position, both the entry and exit points lie on the stock profile.

The techniques used for this cutting mode is an extension of the method used for down/up milling (Fig. 15). The stock profile is first approximated with a step-wise profile (Fig. 15(a)). The stock width of each step is then calculated relative to the outer bound of the swept area. It should be noted that because of the change of the profile direction, the stock widths for

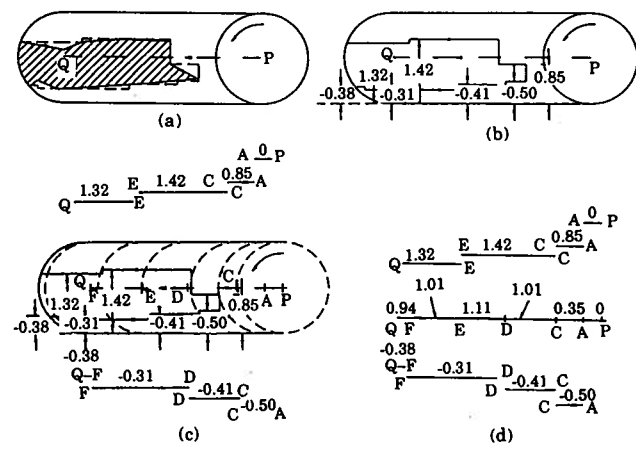


Fig 15 The stock widths with negative values.

lower part steps of the profile are represented by negative values (Fig. 15(b)). Then the original CL segment (from P to Q) is split into small segments according to the upper and lower parts of stock steps separately. Two chains of small CL segments for the lower and upper parts of the stock steps are obtained (Fig. 15(c)). Next, these two chains are merged by combining the widths of the two sides in such a way that each newly generated CL segment can accommodate only one constant width of cut for either side, the actual width of cut is derived by summing up the stock widths of the both sides. The resultant chain is shown in the middle of Fig. 15(d). When the cutter centre moves from P to A, the width of cut is 0; from A to C, the value is 0.35; from C to D, it is 1.01 and so on.

This method can be applied for pro-down-milling and pro-up-milling as well. For slotting, the width of cut can be assumed as the cutter diameter.

**(b) Width of Cut for Combined Cutting Modes**

Sometimes, more complicated CGDs may be encountered, combined cutting modes could occur, such as the both-sides cutting which is shown in Fig. 16. The calculation of the effective width of cut for combined cutting modes can be divided into sub-procedures to calculate the width of cut in simple cutting modes, i.e. analysing the stock areas enclosed in the swept area separately. The final effective width of cut can then be calculated by merging chains of width of cut corresponding to different stock areas. In Fig. 16 it can be seen that the two stock profiles are replaced by step-wise profiles (Fig. 16(a)). The chain of the width of cut for the lower stock area (in down-milling mode) is shown in Fig.16(b), i.e. the corresponding widths for chain PABCQ are 0, 0.27, 0.63, 0.44. The chain of the width of cut for the upper stock area (in up-milling mode) is shown in Fig. 16(c), i.e. the corresponding widths for chain PDEFGQ are 0, 0.31, 0.48, 0.19, 0. Then the result chain of width of cut is shown at the bottom of Fig. 16(d). The widths

of cut when the cutter moves along PADBEFCGQ are 0, 0.27, 0.58, 0.94, 1.11, 0.82, 0.63, 0.44 respectively.

**AN EXAMPLE**

In Fig. 17, a few machined graphs are illustrated to show the progress of the machining. Fig. 17(a) shows the pocket dimensions. Fig. 17(b) shows the computer model and the feature recognised. Fig. 17(c) displays the tool path generated when the cutter diameter (D) is 14 and the stepover (b/D) is 0.8. From Fig. 17(d) to Fig. 17(f), the machined graphs derived during the cutting process are shown. Finally, the simulation result is illustrated in Fig. 17(g). During the derivation of the machined graph, the actual radial width of cut is calculated and recorded, as shown in Table 3.

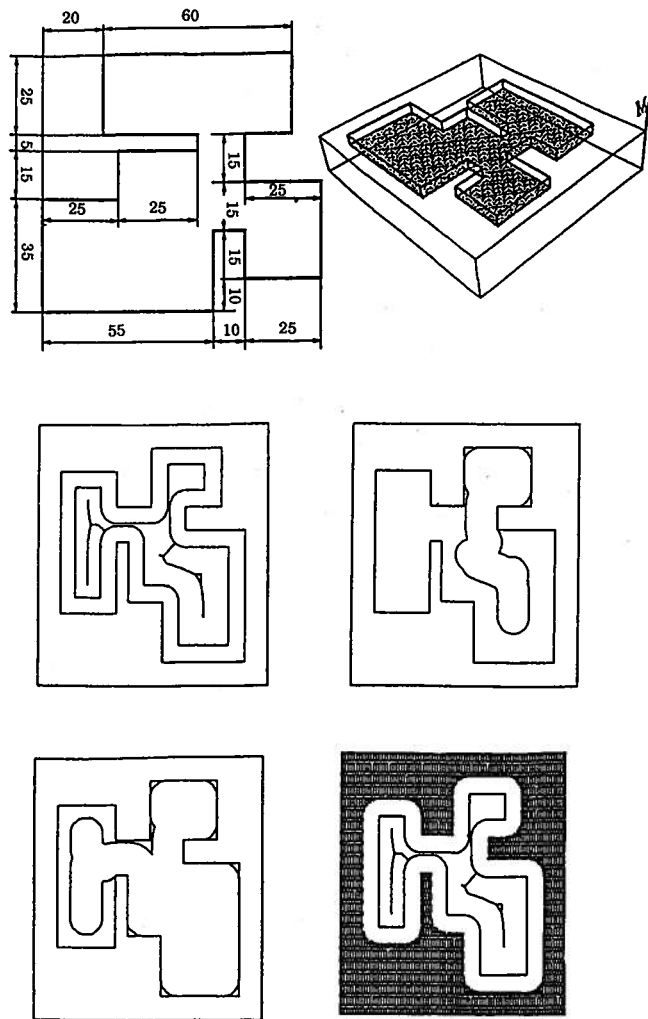


**Fig 17(a)** Dimensions of a example pocket.  
**(b)** Geometrical model and recognised feature.  
**(c)** Tool path generated (D=14, b/D=0.8).  
**(d)** A instant machined graph when simulating the cutting.  
**(e)** A instant machined graph when simulating the cutting.  
**(f)** A instant machined graph when simulating the cutting.  
**(g)** Final result after simulation.

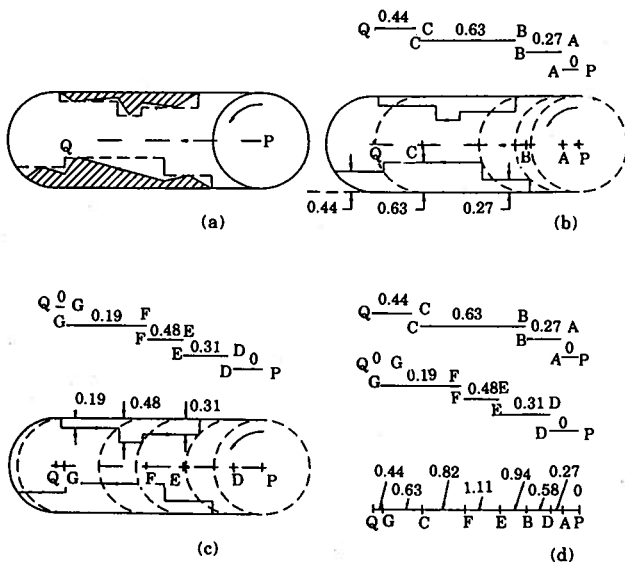


**Fig 16** The calculation of the actual radial width of cut when both-sides cutting is being carried out.



**Table 3(a)** Curve types, cutting modes and the actual radial widths for tool path segments (after being split).

Pass No.	Curve type	Cutting mode	Actual width	Pass No.	Curve type	Cutting mode	Actual width	Pass No.	Curve type	Cutting mode	Actual width
.....				.....				.....			
17	1	1	14.00	61	1	3	8.02	105	2	3	7.00
18	1	3	11.60	62	1	1	14.00	106	1	3	8.00
19	1	1	14.00	63	1	1	14.00	107	1	1	14.00
20	1	3	9.72	64	1	3	8.072	108	1	1	14.00
.....				.....				.....			

**Table 3(b)** Travel distances under different cutting modes and the total travel length.

Mode	Length	Mode	Length
1	401.345	4	188.344
2	10.202	5	1.659
3	477.257	6	0.000
Total length = 1078.807			

Note:

Curve type: 1=straight line, 2=Circular arc;

Cutting mode: 1=Slotting, 2=Up-milling, 3=Down-milling, 4=Symmetrical Milling, 5=Pro-up/down milling, and 6=Not used.

## CONCLUSION

In this paper a simple method to calculate the actual width of cut and to predict the effective cutting mode is presented. Basically, it is based on 2-D simulation of the machined area, and analysis of the cutting geometry diagram. This makes it possible to optimize pocketing operations more precisely and to achieve dynamic optimisation of cutting conditions.

## REFERENCE

- Bouzakis, K. D., Efstathiou, K. and Paraskevopoulou, K. (1992). NC-Code Preparation with Optimum Cutting conditions in 3-Axis Milling, *Annals of the CIRP* Vol. 41/1.
- Hook, T. V. (1986). Real Time Shaded NC Milling Display, *Computer Graphics*, Vol. 20, No. 4, Association for Computer Machinery, 15-19.
- Kline, W. A., Devor, R. E. and Lindberg, J. (1982). Prediction of Cutting Forces in End Milling with Application to Cornering Cuts, *International Journal of Machine Tool Design and Research*, Vol. 22.
- Lau, T. L. (1987). Optimization of Milling Conditions, Ph.D Thesis, University of Manchester, UK.
- Takata, M. D., Tsai, M. I. and Sata, T. (1989). A cutting Simulation System for Machinability Evaluation Using a Workpiece Model, *Annals of CIRP*, Vol. 38/1.
- Wang, K. K. (1987). Application of Solid Modelling to Automate Machining Parameters for Complex Parts, *Proc. of CIRP Manufacturing Seminar*, Penn State, USA, 33-37.

Wang, W. P. and Wang, K. K. (1986). Geometric Modelling for Swept Volume of Moving Solids, *IEEE C G & A*, December.

Wang, W. P. and Wang, K. K. (1986). Real-time Verification of Multi-axis NC programs with Raster Graphics, *Proc. of IEEE Int. Conf. on Robotics & Automation*, the Sanfrancisco Hilton and Tower, Sanfrancisco, April 7-10.

Wang, W. P. (1988). Solid modelling for optimizing Metal Removal of Three dimensional NC End Milling, *Journal of Manufacturing System*, Vol. 7, No. 1.